Assessing Coal Bumps From Excess Energy in Finite Difference Models

Ryan Garvey, Ph.D. Student
Ugur Ozbay, Professor
Mining and Earth Systems Engineering
Colorado School of Mines
Golden, CO

ABSTRACT

A numerical investigation is made into unstable failures of coal pillars (i.e. coal bumps) using the finite difference software FLAC3D. A static energy balance is first derived to calculate the excess energy released as a consequence of unstable failure in rock. Two- and three-dimensional mining layouts are then assessed on their bump-potential based on the magnitudes of excess energy released during simulated pillar failures. A three-dimensional pillar model is developed to represent tributary area loading of an infinite room-and-pillar layout. Pillar strength and brittleness characteristics are calibrated using a Mohr-Coulomb strain-softening constitutive law to simulate width-to-height ratio coal pillars ranging from 1:1 to 5:1. Width-to-height ratio pillars 1:1 to 3:1 release large magnitudes of excess energy as the pillars fail, representing massive collapse of room-and-pillar layouts. The larger pillars maintain their residual strength during failure; however significant excess energy is still released during temporary reductions in pillar strength. A two-dimensional model is then constructed of a gateroad pillar failing due to elastic rebound of the surrounding rockmass. Soft loading conditions initiate unstable failure for all pillar widths, while the total magnitudes of excess energy increase with the size of pillar being modeled. The results from these tests indicate that excess energy may be used as a direct assessment of the bump potential of simulated mine layouts.

INTRODUCTION

Coal bumps and rockbursts are low frequency, high impact unstable failures that pose a serious threat to miners and to the integrity of mine workings. Current numerical modeling software offers capabilities that can be utilized to detect and quantify coal bumps in coal mine layouts. This paper presents a methodology that was developed for assessing the magnitude of unstable failures in simulated FLAC3D mine models.

EXCESS ENERGY BALANCE

During unstable failure, more potential energy is released from a rock system than is stored as strain energy and is consumed through plastic deformation. The resulting excess energy is not accounted for statically and is instead converted into kinetic energy through the dynamic motion of rock within the system. The total kinetic energy released by an unstable failure may thereby be determined from the excess energy of the otherwise static system. This concept is demonstrated for a simple uniaxial compressive strength (UCS) test shown in Figure 1 where a stiff loading system elicits a stable failure while a soft loading system provides excess energy that is then converted into kinetic energy as the brittle specimen is caused to fail in an unstable manner.

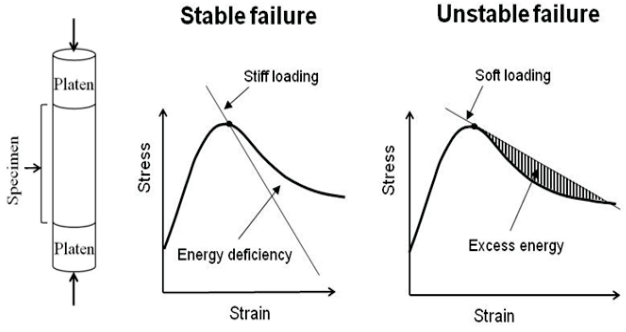

Figure 1. Idealized representation of unstable failure and excess energy in UCS test case.

This concept of excess energy was extended to the more complex loading conditions found in underground mines by calculating the static contributions of energy for a continuum numerical method. The calculation of excess energy, E_e, is shown below where W_b is the total boundary work applied to the system, W_g is the contribution of gravitational potential energy, U is the elastic strain energy stored in the rock, and W_r is the work performed through plastic deformations of the rock. The energy balance is based on Salamon's previous work (1984) and was implemented in FLAC3D v4.01 to determine the total excess energy released during simulated unstable failures.

$$E_e = \left(W_b + W_g\right) - \left(U + W_r\right)$$

A routine was written using the FISH programming language within FLAC3D to calculate boundary work and changes in

gravitational potential energy. The built-in energy tracking module in FLAC3D was then used to calculate the elastic strain energy and the work performed by plastic deformations in the model (Itasca, 2012).

Figure 2 shows the stress-strain results of stable and unstable failures of FLAC3D simulated laboratory triaxial compressive strength tests. Each confinement test was repeated using both stiff and soft loading platens to produce stable and unstable failures, respectively. When the failure is unstable, the specimen stress response follows the elastic rebound of the testing machine as represented by the dashed lines in the plot. If the failure is stable, the specimen compression follows the characteristic post-peak behavior of the specimen. The area between the dotted and solid line in the post-peak regime is proportional to the excess energy released in the case of unstable failures.

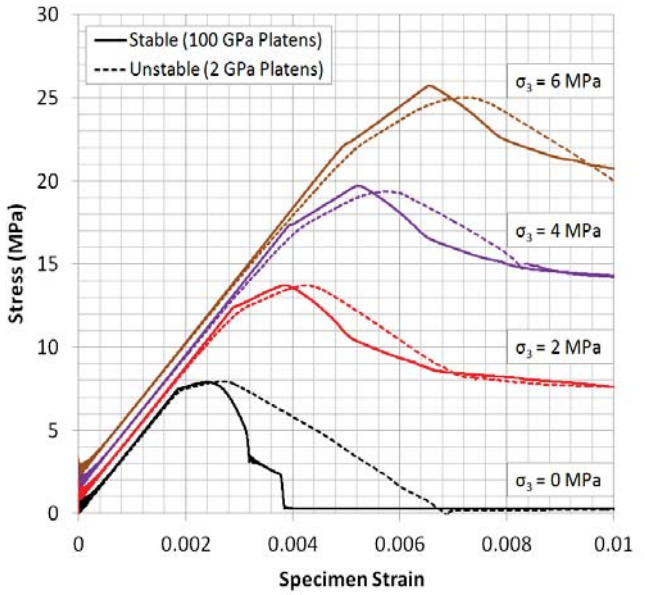

Figure 2. Unstable and stable failures of triaxial compressive strength tests at different confinements.

To demonstrate the proposed approach for determining the excess energy in Figure 2, a set of uniaxial compressive strength tests were run in FLAC3D using the material properties listed in Table 1. First, a pair of stiff 100 GPa platens was used to fail a brittle rock specimen in a stable manner. The results of the energy balance in this case are shown in Figure 3 where the calculated excess energy remained low throughout the test. Next, a pair of soft 2 GPa platens was used to cause unstable failure of the specimen, and the resulting energy histories are shown in Figure 4. In this unstable case, the excess energy increased during the specimen failure and matched expected values of energy released from the unstable system.

THREE-DIMENSIONAL TRIBUTARY AREA MODELS

As shown in the previous section, available constitutive models simulate the stress-strain response of brittle rock while approximating the elastic and plastic energy stored or consumed during failure. Mine models may be constructed using these techniques to allow for unstable failure conditions to arise within

Table 1. FLAC3D inputs for uniaxial and triaxial compressive strength test specimen.

Specimen Geometry	Cylinder, 2m (H) x 1m (D)
Mesh Type/Resolution	Radial, 0.1m (vertical), 0.1m (radial)
Elastic Properties	4 GPa (E); 0.2 (v)
Cohesion vs. Plastic Millistrain	2.41 MPa, 0.5; 0.5 MPa, 9; 0.25 MPa, 15.5
Friction Angle vs. Plastic Millistrain	0°, 0; 15°, 1; 15°, 7; 5°, 12
Dilation Angle vs. Plastic Millistrain	0°, 0; 15°, 1; 15°, 7; 5°, 12

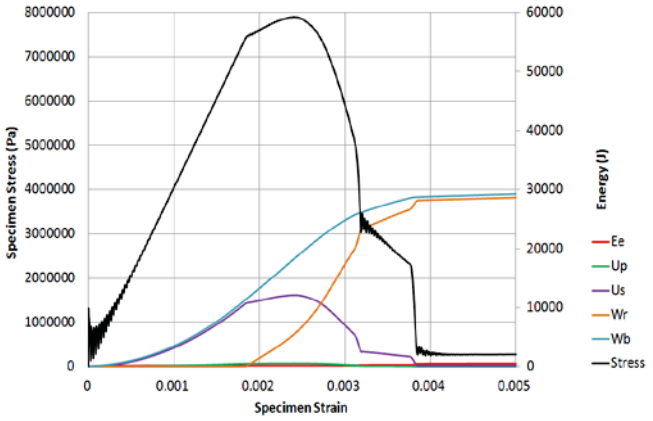

Figure 3. Energy histories of stable UCS test with 100 GPa platens.

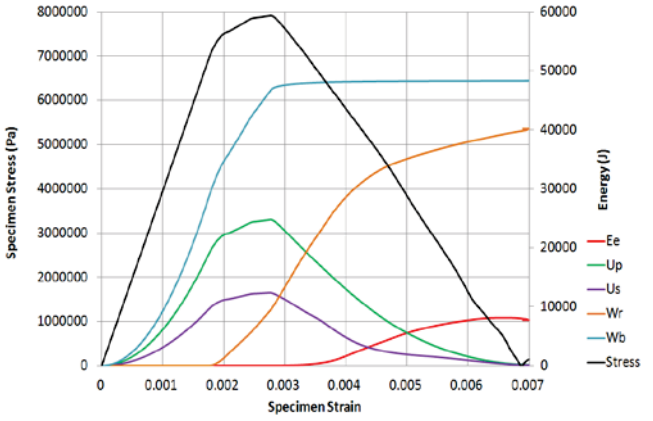

Figure 4. Energy histories of unstable UCS test with 2 GPa platens.

simulated volumes of brittle rock. The explicit representation of failure given by FLAC3D allows for static energy calculations to be performed even while the system is unstable. The total excess energy may therefore be determined during simulated rock failure to provide an assessment of the bump potential of a given mine layout.

The calculation of excess energy was implemented within a quarter-symmetry model of a pillar which represents an infinite room-and-pillar layout. Pillar geometries with width-to-height

ratios from 1:1 to 5:1 were tested under these conditions to determine the excess energy released in each case. A coal seam height of 2.4 m and an entry width of 6 m was assumed for the tests. The resulting model geometry is shown in Figure 5.

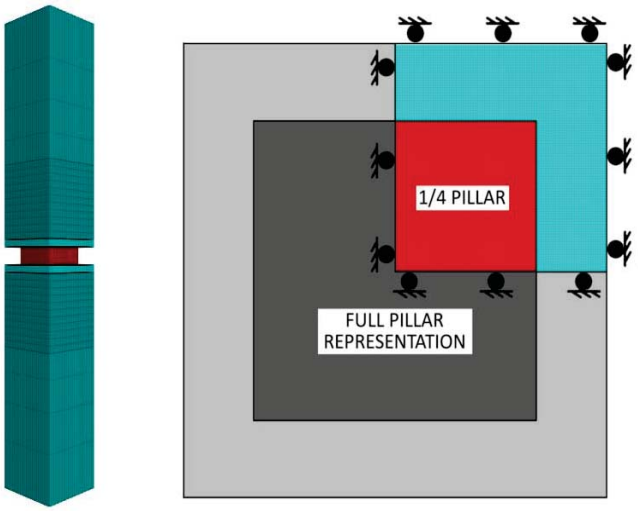

Figure 5. Quarter-symmetry pillar model to represent an infinite room-and-pillar mining layout.

A calibration procedure was applied to the simulated coal pillars to determine appropriate inputs for cohesion, friction angle, and dilation angle in the Mohr-Coulomb strain-softening model (MCSS) found in Table 2. The ultimate strengths of the pillars were compared against the Bieniawski (1968) and Salamon-Munro (1967) pillar strength formulas for a 6.2 MPa cubic strength of coal as shown in Figure 6. The post-failure modulus of the 2:1 and smaller pillars was also assessed against Wagner's classic in situ pillar tests (Wagner, 1974). The calibrated pillar responses shown in Figure 7 were found to be within acceptable ranges for all pillar widths that were tested.

Table 2. FLAC3D inputs for coal pillar models.

Mesh Type/Resolution	Cubic zones, 0.1m^3
Elastic Properties	2.7 GPa (E); 0.12 (ν)
Cohesion vs. Plastic Millistrain	1.45 MPa, 0; 1.45 MPa, 0.5; 0.2 MPa, 21.3
Friction Angle vs. Plastic Millistrain	23°, 0; 30°, 0.5; 30°, 1
Dilation Angle vs. Plastic Millistrain	2°, 0; 10°, 0.5; 10°, 21.3

Gravity was applied to the system and a pressure boundary was established at the top of the model to represent a tributary area load on the pillar. The pressure boundary was increased at a rate of 1 kPa per 100 steps until the pillar was caused to fail. Excess energy was calculated during these tests to assess the magnitudes of energy released due to unstable collapse of the room-and-pillar layouts.

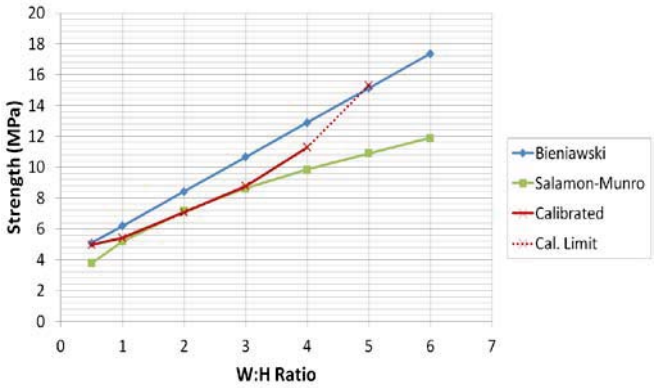

Figure 6. Ultimate pillar strengths of calibrated coal pillars compared against classic coal pillar strength formulas.

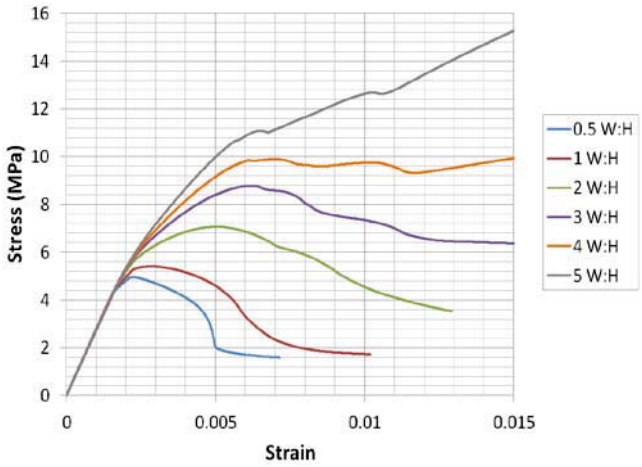

Figure 7. Stress vs. strain histories of the calibrated FLAC3D pillar models.

THREE-DIMENSIONAL MODEL RESULTS

The role of gravitational potential energy was studied in the expression of unstable failure in the quarter-symmetry pillar models. The 1:1 to 3:1 pillars failed in a completely unstable manner that resulted in the unchecked downward displacement of the overburden. An example of the excess energy history is provided for the smallest 1:1 pillar in Figure 8.

The 4:1 and 5:1 pillars were wide enough to maintain sufficient residual strength during failure to resist total collapse of the roof, however the formation of large shear failures in the wide pillars still resulted in temporary reductions in strength and subsequent losses of stability. This concept is demonstrated for the 4:1 pillar in Figure 9 in which a small decrease in strength led to a significant increase in excess energy.

Figure 10 shows the excess energy histories for the different pillar geometries normalized over the total development area. Larger magnitudes of normalized excess energy were recorded for the 1:1 through 3:1 pillars. The 4:1 and 5:1 pillars also showed some increase in excess energy as a consequence of large shear failures within the pillars.

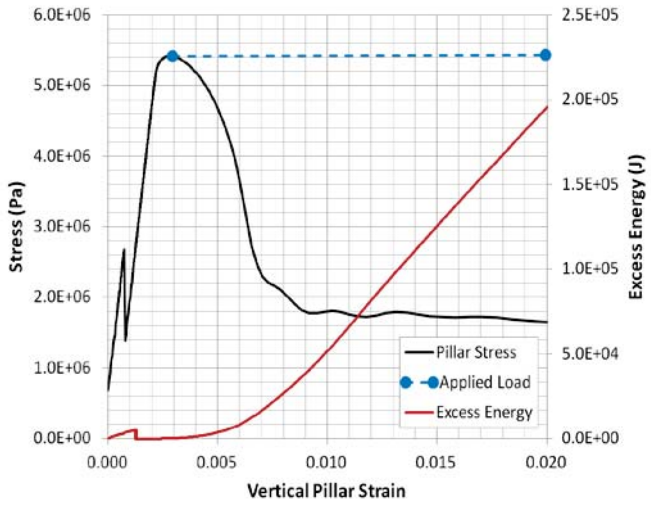

Figure 8. Excess energy during unstable collapse of 1:1 pillar.

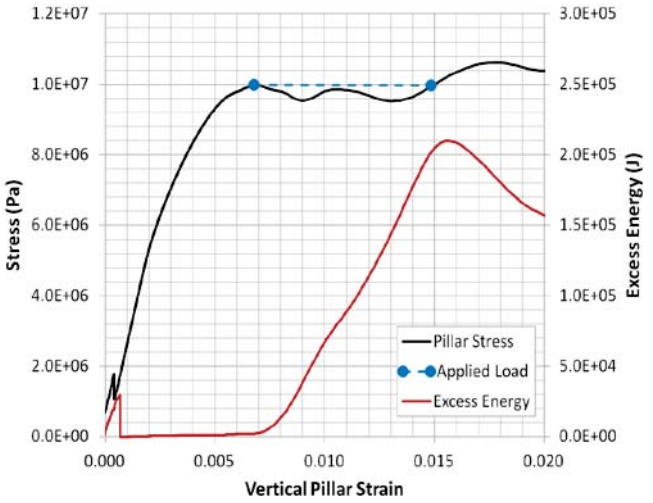

Figure 9. Excess energy during failure of 4:1 pillar.

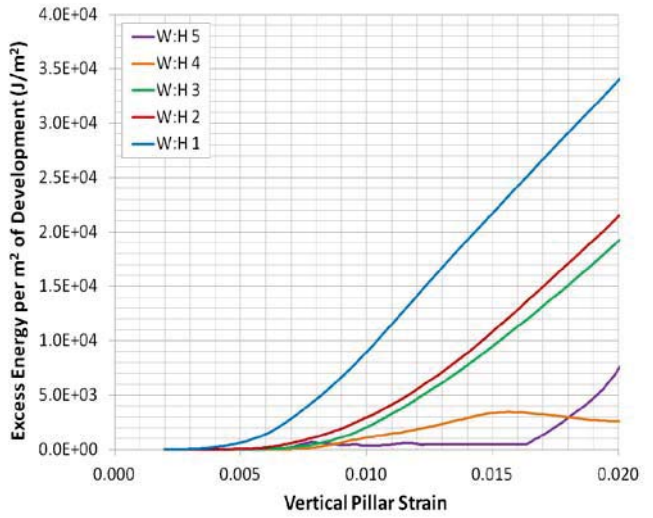

Figure 10. Excess energy released per square meter of development for different pillar geometries.

The calculation of excess energy was shown to be a direct assessment of the stability of different room-and-pillar mine layouts. The results of the tests revealed that smaller pillars of widths 1:1 to 3:1 did not provide sufficient residual strength to resist downward displacement of the roof, and a massive collapse was observed in these cases. The larger pillars led to more stable layouts; however, excess energy was still released due to temporary reductions in residual strength.

TWO-DIMENSIONAL GATEROAD PILLAR MODELS

To study the excess energy levels in the case of a gateroad pillars, a two-entry gateroad layout was assessed for pillar widths ranging from 1:1 to 5:1. The half-symmetry plane strain model shown in Figure 11 was constructed in FLAC3D to represent an elastic rockmass loading a single gateroad pillar with two 6-m entries to either side. The material properties of the pillar matched those found in the three-dimensional model listed in Table 2. Loads were increased in the system through a slow, constant velocity boundary at the top and bottom of the model. No gravitational loading was assumed for these simplified tests.

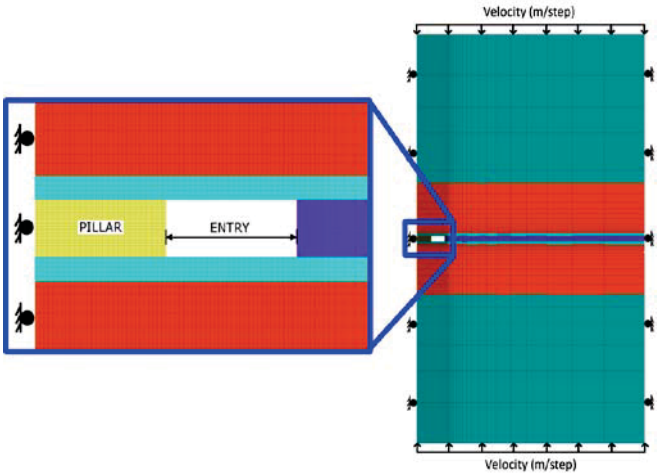

Figure 11. Two-dimensional plane strain model of gateroad pillar.

The elastic modulus of the rockmass was adjusted between tests to allow more or less strain energy to be stored in the loading system prior to the failure of the pillar. Young's moduli of 2, 5, and 20 GPa were assigned to induce unstable (2 GPa), quasi-stable (5 GPa), and stable (20 GPa) pillar failures. The stress-strain results of the 1:1 pillar are shown in Figure 12 where the 2 GPa rockmass led to an unstable failure and a deviation of the post-peak pillar response from expected values.

The results of the excess energy calculations are shown in Figure 13 for all test cases. Excess energy magnitudes increased with increasing widths in the unstable 2 GPa rockmass. These results revealed that more energy was released due to unstable failure conditions within the stronger, wide pillar cases.

The failure mode of the pillar played an important role in the stability of the simulated gateroads. Stress and strain measurements could be used for the smaller 1:1 and 2:1 pillars to directly identify the presence of unstable failure conditions however this approach became unsuitable for wider pillars which

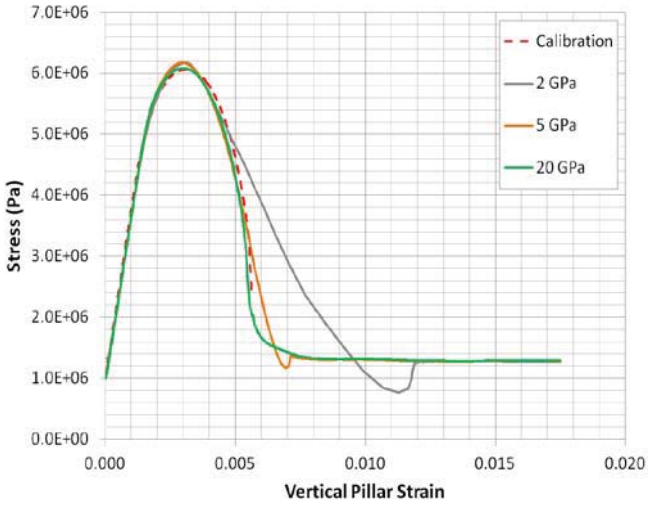

Figure 12. Failure of 1:1 pillar by unstable 2 GPa, quasi-stable 5 GPa, and stable 20 GPa rockmass conditions.

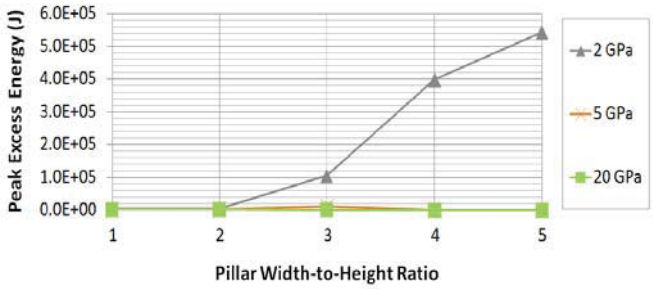

Figure 13. Excess energy released in gateroad models for increasing width-to-height ratio pillars.

experienced complex, multi-stage failure modes. The calculation of excess energy provided the only direct assessment of unstable failure and bump-potential for the wider pillar geometries of 3:1 and greater. A more thorough discussion of the changing failure mode of pillars at different width-to-height ratios is provided in Garvey's analysis (2013).

CONCLUSIONS

The excess energy calculation provided a rational method for analyzing the bump potential of room-and-pillar and gateroad layouts. During tributary area loading of the three-dimensional models, the smallest pillar geometries released the highest magnitudes of excess energy as is consistent with the scenario of a massive collapse of undersized pillars. In the two-dimensional gateroad, the excess energy increased with increasing pillar widths for the unstable, soft rockmass conditions.

Additional testing of the energy balance is required to calibrate the plastic work consumed during unstable pillar failure to match the approximate values of in situ pillar failures. Future backanalysis studies should also be conducted to validate the magnitudes of excess energy in the FLAC3D models against measures of the total kinetic energy released in historical cases of coal bumps.

REFERENCES

Bieniawski, Z.T. (1968). "In situ strength and deformation characteristics of coal." Engineering Geology, vol. 2: 325-340.

Garvey, R. (2013). "A study of unstable rock failures using finite difference and discrete element methods." PhD Thesis. Golden, CO: Colorado School of Mines, pp. 147–190.

Itasca Consulting Group Inc. (2012). FLAC3D Online User's Manual Version 5.0. Minneapolis, MN: Itasca Consulting Group Inc., pp. 1–35; 1–36.

Salamon, M.D.G. and Munro, A.H. (1967). "A study of the strength of coal pillars." Journal of the South African Institute of Mining and Metallurgy, September 1967, pp. 55-67.

Salamon, M.D.G. (1984). "Energy considerations in rock mechanics: Fundamental results." Journal of the South African Institute of Mining and Metallurgy. 84(8): 233–246.

Wagner, H. (1974). "Determination of complete load deformation characteristics of coal pillars." In: Proceedings of 3rd ISRM Congress. International Society for Rock Mechanics, pp. 1076 – 1081.